We are IntechOpen, the world's leading publisher of Open Access books
Built by scientists, for scientists

6,900
Open access books available

186,000
International authors and editors

200M
Downloads

Our authors are among the

154
Countries delivered to

TOP 1%
most cited scientists

12.2%
Contributors from top 500 universities

CLARIVATE ANALYTICS
BOOK CITATION INDEX
INDEXED

WEB OF SCIENCE™

Selection of our books indexed in the Book Citation Index in Web of Science™ Core Collection (BKCI)

Interested in publishing with us?
Contact book.department@intechopen.com

Numbers displayed above are based on latest data collected.
For more information visit www.intechopen.com

13

Laser-Induced Autofluorescence as a Possible Diagnostic Tool for Use in Neurosurgery

Mihail - Lucian Pascu[1], Mihaela - Oana Romanitan[2], Alexandru Pascu[1], Josè - Maria Delgado[3] and Leon Danaila[4]

[1]*National Institute for Laser, Plasma and Radiation Physics, Laser Department, Bucharest*
[2]*Neurology Clinics, Emergency University Hospital, Bucharest*
[3]*Division de Neurociencias, Universidad Pablo de Olavide, Sevilla*
[4]*Neurosurgery Clinics, National Institute of Neurology and Neurovascular Diseases, Bucharest*
[1,2,4]*Romania*
[3]*Spain*

1. Introduction

One of the main neurosurgical problem consists in accurately identify the margins of brain tumors to allow a tumor's precise excision without destruction of the surrounding healthy tissue. Excision is optimal if the tumor mass is removed from the brain without affecting the surrounding healthy tissue or with minimum injury to it. The result of resection and the histopathological diagnosis of the extracted tumor tissue impose a therapeutic strategy to further treat the disease. Given these clinical requirements, it is highly recommended to accurately identify tumor tissue borders during the surgical operation proper, by means of specific methods and techniques. Identification is done in two steps: (a) a preoperative imaging of the tumor tissue and borders using CT, MRI, and/or ultrasound-based equipment; and (b) an intraoperative stage, in which the tumor borders are identified by direct visual inspection; the operating microscope, endoscopic techniques, and autofluorescence measurements of the tumor and healthy tissues are also available methods that may be associated with the visual observation/search.

Laser-induced autofluorescence is one of the main candidates for use in the operative field to identify tumor borders in both benign and malignant cases. It may allow, in principle, accurate identification of the interface between normal brain tissue and tumor tissue by measuring the optical fluorescence spectra emitted by these tissues after excitation with laser optical beams having suitable characteristics. Literature reports show that the autofluorescence method is promising for delineating brain tumor resection margins (Bottirolli et al., 1998; Lin et al., 2000; Lin et al., 2001; Croce et al., 2003; Cubillos et al., 2006). At the same time, more research needs to be devoted in order to develop the instruments, procedures, and clinical recommendations for intraoperative use of autofluorescence, at the level of both in vivo and in vitro measurements (Kremer et al., 2009).

Literature reports also show that progress was made stepwise to identify brain tumor tissues and to differentiate them from the normal brain tissues on the base of the laser induced fluorescence emitted by exogenous fluorophores (K. Svanberg and S. Svanberg 1983, J. Ankerst et al.1984, S. Montan, K. Svanberg and S. Svanberg 1985, K. Svanberg 1986, Andersson – Engels et al. 1989, 1994). An alternative is the measurement of the autofluorescence emitted by the brain tissues, i.e. by the endogenous fluorophores contained naturally in them. The autofluorescence experiments were approached and are still developed along two main lines: the measurements of the spectral properties of the autofluorescence beams and the contemporary or consecutive measurements of the lifetime of the autofluorescence radiation (Andersson-Engels, et al. 1990a,b, Marcu et al. 2004, Butte et al. 2011). Combinations of these techniques reflected in imaging spectroscopy are also experimented (Gebhart et al. 2006, Kantelhardt 2007, Butte et al. 2010, Sun et al. 2010).
This book chapter is conceived as a synthesis of the characteristics of the laser-induced autofluorescence method applied in neurosurgery for diagnostics and/or intraoperative procedures; at the same time relevant research contributions of the authors in this field are described in more detail and discussions are made on the place occupied by the autofluorescence method among the other methods/techniques used for real time differentiation between normal and tumor brain tissues.

2. Materials and methods

2.1 Autofluorescence definition: basic data

The autofluorescence emitted by a tissue (in particular the brain tissue) is that fluorescence emitted by it when exogenous fluorescent substances are not added to it; in other words the autofluorescence radiation is emitted only by the natural constituents of the tissue when an optical radiation of suitable wavelength falls on the tissue. Consequently, autofluorescence spectra give accurate information about the content and molecular structure of the emitting tissue. The autofluorescence is emitted by molecules that exist normally in the tissues, following their resonant interaction with optical radiation. The scheme that describes the fluorescence emission and the lifetime of the fluorescence radiation emitted by a molecule (usually named fluorophore) is shown in Fig.1 (Danaila and Pascu, 2001; Valeur, 2001).
The molecular de-excitation may also involve the energy transfer from an excited electronic singlet state to an excited triplet state by the process called "intersystem crossing", one system being formed by the singlet and other by the triplet states (v=0 of S_2 to v=4 of T_2, or v=2 of S_1 to v=0 of T_2, or v=0 of S_1 to v=4 of T_1). The de-excitation of the molecule may be also produced without changing the electronic state by passing without emission of radiation from excited vibrational levels to less excited vibrational levels; this process being called vibrational relaxation and is accompanied by the slight heating of the samples.
If the fluorophore interacts with an optical radiation emitted by an external light source in visible and/or ultraviolet, then the first process which takes place is the absorption of one (transition S_0 to S_1) or more (transition S_0 to S_1 followed by S_1 to S_2 etc) photons of this pumping radiation and the consequent excitation of the molecule due to the transition selection rules from the fundamental singlet state S_0 to the S_1, S_2,…S_n states; the time interval needed for that is one fsec i.e. the process is so fast that the excitation of the molecule takes place so quickly that the nuclei are found in the same position before and after the transition. Once excited on a vibrational (or rotational-vibrational) state of an excited singlet state, the molecule may pass to the fundamental singlet state on different

vibrational levels in different ways (Brewer et al., 2001). One is the internal conversion on the S_1 state which takes place in 10^{-6}s – 10^{-12}s followed by vibrational relaxation in 10^{-12}s – 10^{-13}s on the v=0 vibrational level of the S_1 excited singlet state. Both processes are nonradiative and the energy lost by the molecule is transformed in kinetic energy of it that may slightly increase the tissue temperature. From v=0 of S_1 the molecule falls radiatively on several vibrational levels of the S_0 state emitting fluorescence radiation in 10^{-6}s – 10^{-9}s. This is the main way in which the autofluorescence radiation is emitted, so that its characteristics such as wavelength, spectral range, time duration, polarization state are specific to the emitting molecules; i.e. the fluorescence radiation properties are related to the structural properties of the emitting molecules and with their environment which may influence the fluorescence emission. From the S_1 state the fluorophore molecule may decay with a much lower probability back to the S_0 fundamental singlet state by other mechanisms.

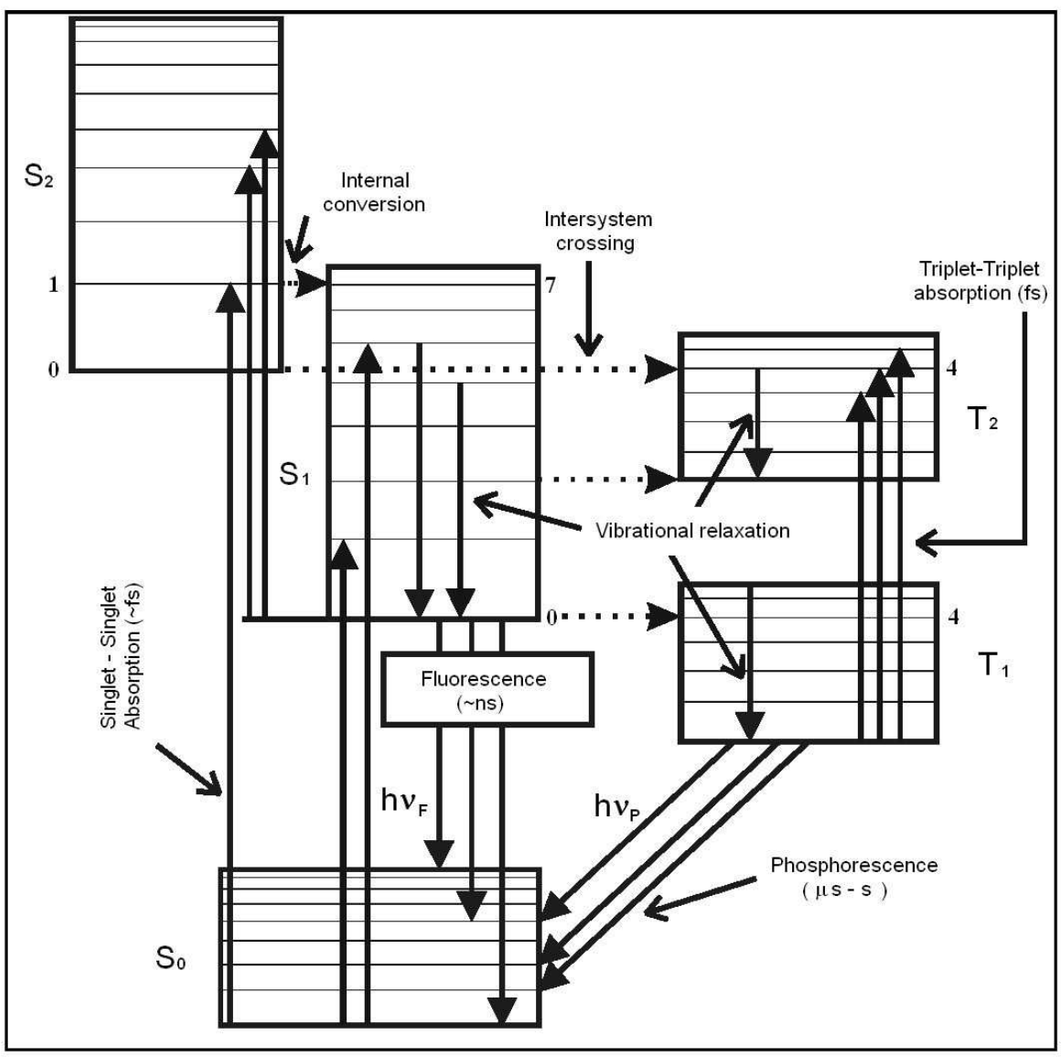

Fig. 1. Molecular diagram used to describe the emission of fluorescence radiation

The molecule may pass from the S_1 state to the first excited triplet state T_1 by intersystem crossing in 10^{-4}s – 10^{-13}s; so, the molecule may occupy a vibrational level of a triplet state after which a vibrational relaxation may occur in 10^{-12}s – 10^{-13}s at the end of which v=0 on T_1 state is populated. The first triplet state T_1 of the fluorophore molecule is metastable and consequently the lifetime of the molecule on it is much longer than on S_1. From it there are two possibilities for the molecule to further de-excite. One is the radiative transition on different vibrational levels of the fundamental singlet state S_0 which leads to the emission of phosphorescence radiation at longer time intervals than the fluorescence radiation with respect to the time moment at which the S_0 – S_n absorption occurs; usually, the phosphorescence takes place in 10^{-4}s – 10^{-2}s which is the lifetime of the molecule on the T_1 state. The phosphorescence radiation also differs from the autofluorescence by the wavelengths which are always longer in phosphorescence than in the fluorescence case.
The second possibility to de-excite T_1 to the S_0 state is the intersystem crossing process ($T_1 \rightarrow S_0$) followed by fluorescence quenching which takes place in 10^{-11}s–10^{-12}s. The fluorescence quenching is, in fact, the process of vibrational relaxation which leads to the nonradiative decay of the molecule on v=0 belonging to the S_0 singlet state.
As a rule, the autofluorescence emission is produced after absorbing one photon of radiation at a wavelength which is usually in the near UV or in the short wavelengths range of the visible. Due to the fact that the fluorophore molecules are surrounded by the other tissues components, which normally (but not only) act as a liquid environment of the molecules, the rotational-vibrational levels are broadened on the singlet and triplet states so that the absorption and the fluorescence emission spectra are broad and their structures are also broadened. Consequently, in the autofluorescence spectra a partial superposition between the emitted bands takes place but, nevertheless, the spectra characteristics are specific to the emitting molecules. At the same time, the fluorescence spectra ($S_1 \rightarrow S_0$ transitions) are more or less the mirror images of the corresponding absorption spectra. The pH of the tissue in which the emitting molecules are embedded may also influence the autofluorescence spectra characteristics, such as the spectral width, the shape etc. Some of the molecules found in the tissue alongside with the emitting fluorophores may absorb the emitted fluorescence; this leads to autofluorescence decrease and from here to errors in measuring/estimating the emitters' positions and concentrations in the tissue.

2.2 Autofluorescence experimental monitoring

The experimental system for measuring autofluorescence signals should be conceived taking into account that fluorescence excitation is always produced at shorter wavelengths than is the emitted fluorescence radiation. At even longer wavelengths, autophosphorescence is emitted, with a lifetime longer than that of autofluorescence. The spectral distribution of the autofluorescence emission is much broader and more structured than that of the pumping/excitation radiation; at the same time its duration is usually longer than, and its polarization state is different from, that of the pumping beam. The coherence state of the excitation beam is different from that of the autofluorescence radiation. Experimentally, it is possible to excite autofluorescence using a laser beam that is monochromatic, coherent, and highly polarized. The obtained fluorescence radiation is incoherent, broad–band, and nonpolarized.
Autofluorescence measures exclusively the properties of the tissues, because it is produced only by their endogenous molecules. It may provide, mainly, two types of information

(Sokolov et al., 2002): (a) image – allows obtaining a more or less extended image of a part of the studied tissue (Gebhart et al., 2006; Kantelhardt et al.,); and (b) fluorescence radiation – it is excited by focusing the pumping beam on the tissue (Lin et al., 2000, 2001, 2002; Kremer et al., 2009; Pascu et al., 2009). The fluorescence radiation has a spectral distribution and a specific intensity; it also has a polarization state, and is characterized by specific ratios between the spectrum peaks.

Autofluorescence is highly sensitive to endogenous emitters of the tissue, if properly excited. It allows identification of the molecular components of a tissue and their combinations, and investigation of the interaction between them and the surrounding media (usually described by the pH of the tissue); it also allows the monitoring of the modifications produced in the molecular composition of a tissue by the effect of natural and/or artificial factors.

The autofluorescence emission of a fluorophore may be characterized by the following properties (Pascu et al., 2009): overall intensity of the emitted spectrum; emission spectral range; spectral structure of the radiation described by the intensity peaks and their relative ratios and by the wavelength of the main intensity peak (if such peak exists); fluorescence lifetime, measured either by its full time width (FTW) or by the full time width at the half maximum of the fluorescence peak (FTWHM), if only one peak is involved (Yong et al., 2006).

The measurement of the lifetime requires excitation of the autofluorescence with a laser pulse that is short enough, i.e. it should have an FTWHM of 5 ns, at most. This parameter may be measured for each fluorescence peak if the autofluorescence spectrum exhibits more peaks.

Human brain tissues (both normal and tumor) contain endogenous fluorophores that belong to the following classes of biomolecules: aminoacids (tryptophan, tyrosine, phenylalanine); structural proteins (collagen, elastin); enzymes and co-enzymes (flavin adenine dinucleotide - FAD, the reduced form of the nicotinamide adenine dinucleotiode-NADH, flavins); lipids (phospholipids, lipofuscin, ceroids); porphyrins; and vitamins (A, K, and D). The autofluorescence emitted by the tissue contains signals originating from the active fluorophores and depends on their concentration and spatial distribution, as well as the properties of the surrounding environment, such as pH, optical properties, structure and organization, homogeneity, (an)isotropy, and turbidity.

The autofluorescence is, therefore, sensitive to the above mentioned properties, and may signal small modifications of any of them. Moreover, tissue histology and biochemistry leave their signatures on the autofluorescence spectra (Bottiroli et al., 1998; Toms et al., 2005). Consequently, variations in the health state of the tissue that modifies its histology and/or histochemical properties can be evidenced by autofluorescence measurements. Such is the case of tumor/malignant tumor tissues that have properties that differ from those of a normal tissue; autofluorescence may become a method to detect and investigate malignant tumor tissues (Svanberg, 1987).

In neurosurgery, it may assist the neurosurgeon to find, in real time, the borders of the malignant tumors. To do this, specialized equipment should be developed to detect the malignant tumors and/or their limits in the brain for early stages or more-developed tumor tissues.

This article brings together the autofluorescence measurements made by the authors in brain tissues in view of future specific equipment development.

2.3 Sample preparation

2.3.1 First type of sample preparation

This approach was exploratory and it was chosen initially to find the best procedures for sample processing and for their mounting in the optical system. The conclusions that resulted from the measurements were used to identify the conditions for reproducibility in: sample preparation and arrangement in the optical set-up utilized for autofluorescence spectra excitation and collection.

Accordingly, a protocol to conserve, transport, and treat tumor/normal tissues was established, to ensure unaltered samples. Once extracted using operative procedures, the brain tissue samples were kept immersed in natural saline at 20°C in a Dewar container. The time interval between tumor extraction and measurements was, at most, 60 min. The samples were irrigated from time to time with natural saline to prevent uncontrolled drying and to remove blood traces; the control and in any case the removal of the blood traces from the samples are important since blood fluorescence may superpose on the autofluorescence of the sample tissues (Andersson-Engels et al., 1990a,b). The working temperature was 20°C. To ensure the best possible conditions for reproducibility of the measurements and to prevent errors in the fluorescence excitation and collection, the samples were placed in direct contact with an optical quartz plate of 0.5 mm in thickness; each sample surface that was exposed to the excitation / fluorescence pumping radiation and from which the fluorescence was emitted was very well defined. The exposed surface was 1–2 mm in diameter (diameter of the excitation beam), and for each sample 5 such spots/discs were used in the measurements; the geometrical arrangement was reproducible, and the results obtained for each excitation wavelength were averaged.

2.3.2 Homogenate preparation

The results from the studies performed on samples processed as mentioned in the previous paragraph, have shown that there are variations in the reproducibility of the autofluorescence curves. To avoid this, samples were processed using a different method, namely, as homogenates: each sample was washed abundantly in natural saline, then ground and further exposed to ultra-sounds to obtain a homogeneous mixture. The preparing of the homogenates did not affect the molecular structures or concentrations of the constituent fluorophores in the samples. It was done to prevent errors due to the unhomogeneities occurring naturally in the collected samples and to the geometry at the interface between the tissue and the optical excitation/collection system.

The optical arrangement for autofluorescence excitation/ collection was the same as described in the paragraph above. For each measured sample (either tumor or normal tissue), three measuring points/spots were used, and the three signals were averaged. The autofluorescence excitation and detection system worked for all samples within the same spectral range (excitation between 337 and 500 nm, and emission measurement between 400 and 650 nm), so that no corrections related to variation in the sensitivity of the photodetectors with wavelength were needed from one sample to another.

2.4 Experimental set-up and sequence

The main goal of the measurements was to identify the spectral properties of the autofluorescence of brain tissues for two cases/types of samples: normal tissues and malignant tumor; by studying these spectra, one aimed to establish criteria to differentiate

between the fluorescence radiations emitted by the two types of samples and to quantify the differences between them. The experiments were made in two steps: (a) measurement of the spectral characteristics of the autofluorescence emitted by the fluorophores existing in the brain tissues; and (b) comparative in vitro measurements of the spectral properties of the autofluorescence emitted by pairs of normal/malignant tumor tissue.

The experimental set-up (shown in Fig.2) consisted of a system adapted to measure laser-induced fluorescence (LIF).

In choosing the radiation source used to excite the autofluorescence, several variants previously reported in the literature were evaluated (Ramanujam et al., 1994; Ramanujam, 2000; Lin et al., 2002; Wu et al., 2003).

For the purpose of this work, a pulsed laser with emission in the near-ultraviolet and visible spectral ranges was developed. This has two advantages: (a) it generates short time-width laser pulses of relatively low energy, which produce a weak perturbation of the studied tissues and a higher overall efficiency of the fluorescence emission; and (b) it enables measurement not only of the spectral distribution of the autofluorescence radiation but also of the fluorescence emission lifetime.

The laser source is a frequency-doubled tunable dye laser pumped by a nitrogen pulsed laser (NPL), described elsewhere (Danaila and Pascu, 1999; Pascu, 2000; Danaila and Pascu, 2001). The main characteristics of the laser system unit used to pump the fluorescence are (a) NPL: emission at 337.1 nm, laser beam bandwidth < 0.1 nm, pulse FTW 1 ns, energy / pulse 50 μJ, peak power per pulse 500 kW, pulse repetition rate continuously adjustable between 1 and 10 pulses per second (pps), beam divergence 5 mrad x 10 mrad; and (b) tunable dye laser: NPL pumped, emits tunable radiation between 350 and 700 nm by using a succession of dyes, beam spectral bandwidth maximum 0.2 nm, pulse FTW 1 ns, energy per pulse typically 5 μJ, pulse repetition rate as driven by the NPL, and laser beam divergence 5 mrad. The dye laser beam focusing produces an irradiance of 10^8 W/m^2 on the sample. The dyes that were mostly used in the experiments are given in Table 1.

Laser dye	Synonymous	Chemical formula	Molec. weight	Solvent	Molar concentration
POPOP	2,2'-(1,4-phenylene)bis[5-phenyl-oxazole]	$C_{24}H_{16}N_2O_2$	364	toluene	$3.5 \cdot 10^{-3}$
Coumarin 540A (Coumarin 153)	2,3,6,7-tetrahydro-9-(trifluoromethyl)-1H,5H,11H-[1]benzopyrano[6,7,8-ij] quinolizin-11-one	$C_{16}H_{14}F_3NO_2$	309.29	ethanol	$5 \cdot 10^{-3}$
Rhodamine 590-Rh 590 (Rhodamine 6G-Rh 6G)	2-[6-(ethylamino)-3-(ethylimino)-2,7-dimethyl-3H-xanthen-9-yl]-benzoic acid, ethyl ester perchlorate	$C_{27}H_{29}C_lN_2O_7$	543.01	ethanol	$5 \cdot 10^{-3}$

Table 1. Laser dyes used in the autofluorescence experiments

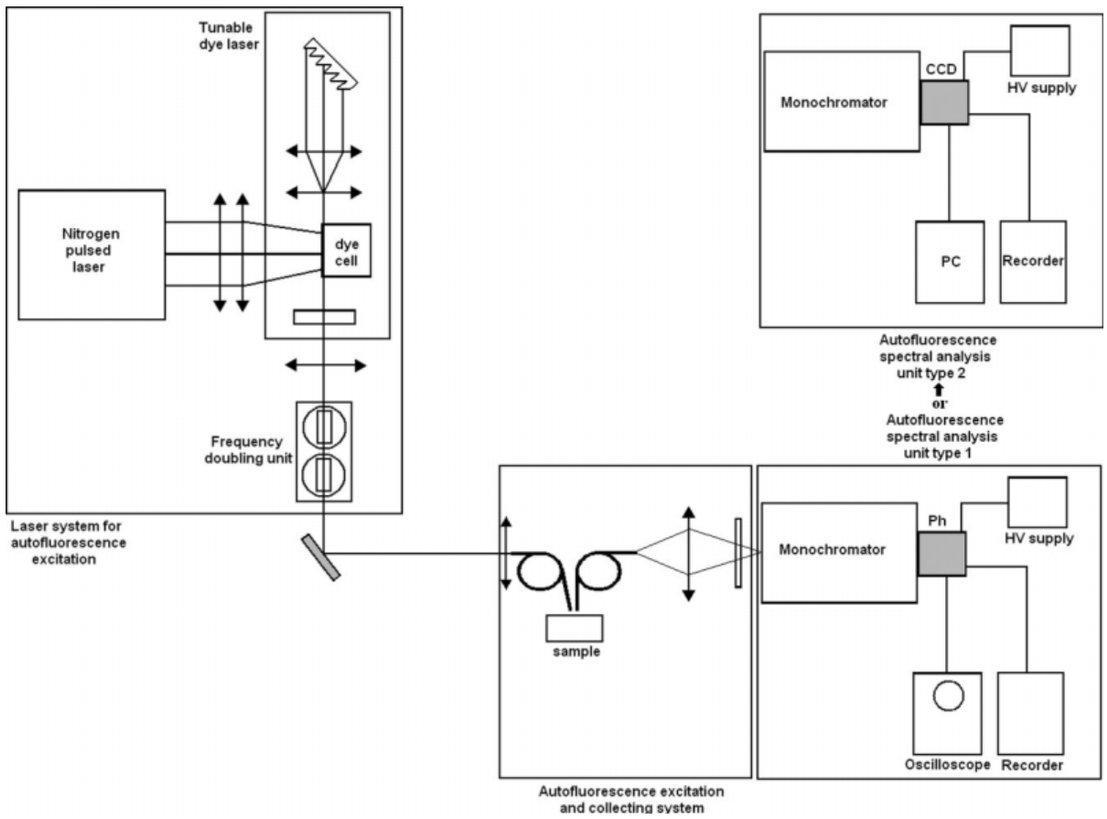

Fig. 2. The fluorescence/autofluorescence excitation set-up.

The frequency doubling crystal used to cover by second harmonic generation (SHG) the wavelength gap in the near-ultraviolet up to 337.1 nm is an ADP crystal; the obtained laser beam has with the following characteristics: tunability range 260 – 300 nm, spectral bandwidth 0.05 nm when the pumping dye laser beam has 0.1 nm full spectral bandwidth, pulse FTW ≤ 1 ns, pulse repetition rate as driven by the NPL, peak energy per pulse typically 0.5 μJ, which enables obtaining a peak irradiance of 5×10^6 W/m^2 at the focus. The system to excite and collect the autofluorescence signal (Fig. 2) consisted of a pair of optical fibers, one of which is used to excite the autofluorescence; it transmits the excitation beam with losses lower than 1%. The excitation optical fiber is a quartz fiber with a core of 1.5 mm in diameter; it has a transmission spectral range between 180 and 700 nm, and a numerical aperture NA = 0.22. The fiber used for the collection of the autofluorescence signal is a fiber bundle of 6 mm in diameter, transmitting between 400 and 700 nm. The sample is either a solution or a piece of brain tissue prepared for in vitro measurements. The autofluorescence radiation transmitted by the collection optical fiber is focused on the input slit of a monochromator; this is part of the spectral analyzing unit, and works between 220 and 800 nm at a linear dispersion of 0.4 nm/mm; signal detection is made by using a fast photomultiplier, sensitive between 180 and 800 nm and able to measure optical signals with rise times of up to 1 ns. With this system (Autofluorescence spectral analysis unit type 1 in Fig.2), the spectral distribution and the lifetime of the autofluorescence were measured.
The second variant (Autofluorescence spectral analysis unit type 2 in Fig.2) for signal detection was a computer- controlled, 2048 pixel CCD camera working between 300 and 800 nm, used only for spectral distribution measurements.

3. Results

3.1 Fluorophore measurements

The measured samples were primary endogenous fluorophores, such as aminoacids, structural proteins, enzymes and coenzymes, porphyrins, and riboflavins. Literature reports (for example Zuluaga et al., 1999; Drezek et al., 2001a, b) on the fluorescence properties of such fluorophores show sets of data measured in experimental conditions that differ slightly from one case to another; this prevents the construction of a reference system based on which the interpretation of the autofluorescence data measured in brain tissues could be made. In this chapter, are presented data measured on primary fluorophores that are potentially present in the brain tissues, aiming to have controllable comparison conditions for the autofluorescence measurements made on tissue samples. So, Figs. 3 – 5 show the fluorescence spectra of the, respectively, phenylalanine, tryptophan and tyrosine solutions are shown when excited at 266 nm.The samples for each substance were phosphate buffer aqueous solutions at pH = 7 and the concentrations were in each case 10^{-5}M.

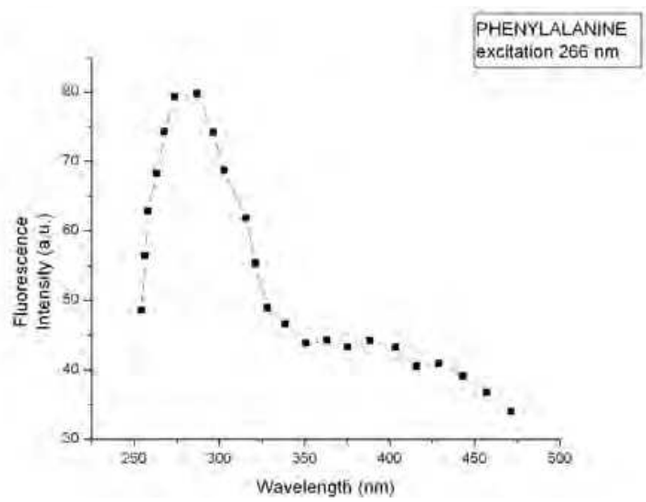

Fig. 3. The phenyalanine fluorescence emission spectrum

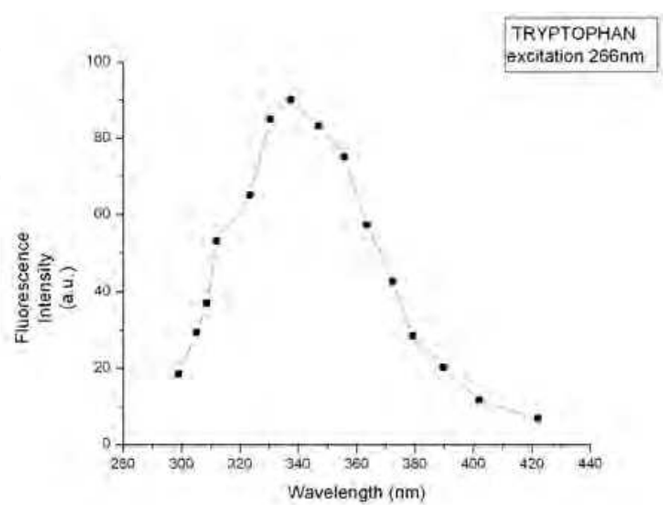

Fig. 4. The tryptophan fluorescence emission spectrum.

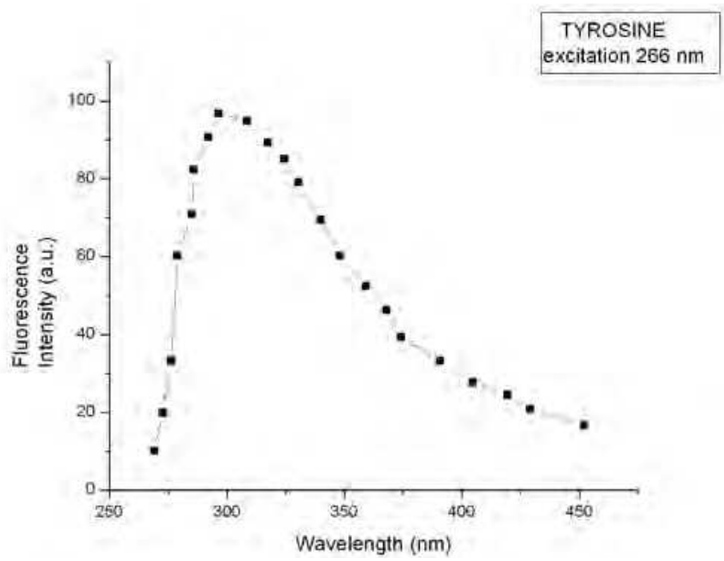

Fig. 5. The tyrosine fluorescence emission spectrum

The fluorescence peaks for each of these aminoacids are broad, have different intensities, are unstructured and constitute a superposition of narrower peaks originating in transitions between several specific pairs of electronic states. To obtain an objective base for the autofluorescence spectra, the LIF was measured for various fluorophores. Figs. 6–12 show fluorescence spectra emitted by fluorophores which are found in brain tissues as follows: in Fig.6 NADH excited at 337.1 nm with NPL laser beam; in Fig.7 and Fig.8 collagen excited at 266 nm with beam obtained by SHG from Rh6G emission at 532 nm, respectively at 337.1 nm; in Fig.9 elastin excited at 337.1 nm; in Fig.10 FMN (flavin mononucleotide) excited at 337.1 nm; in Fig.11 riboflavin excited at 440 nm; in Fig.12 protoporphyrin excited at 440 nm by laser beam emitted either by coumarine or by POPOP.

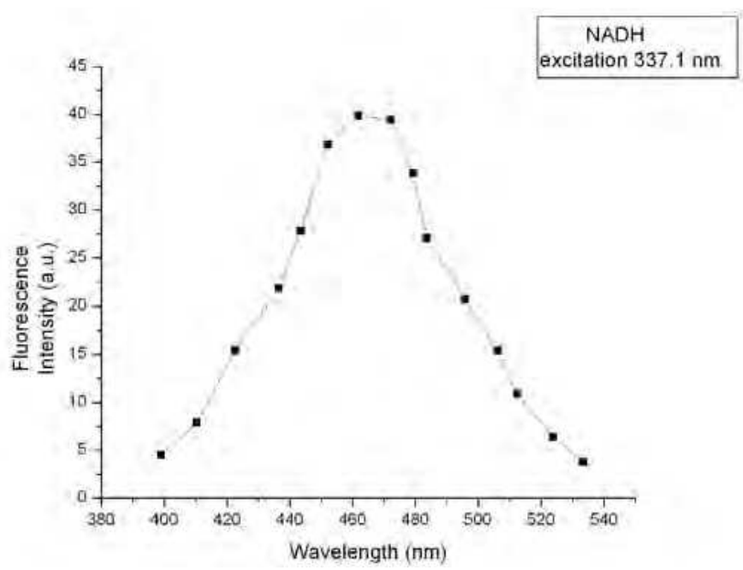

Fig. 6. Fluorescence emission of NADH

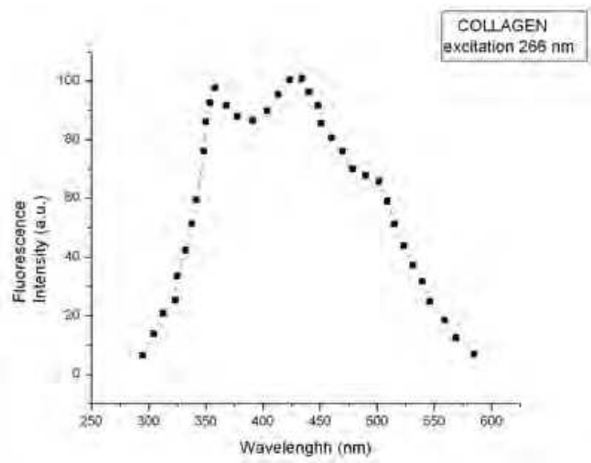

Fig. 7. Fluorescence emitted by collagen excited at 266 nm

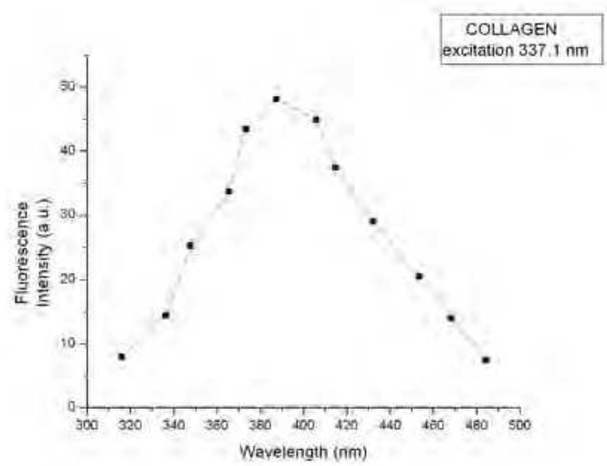

Fig. 8. Fluorescence emission by collagen excited at 337.1nm

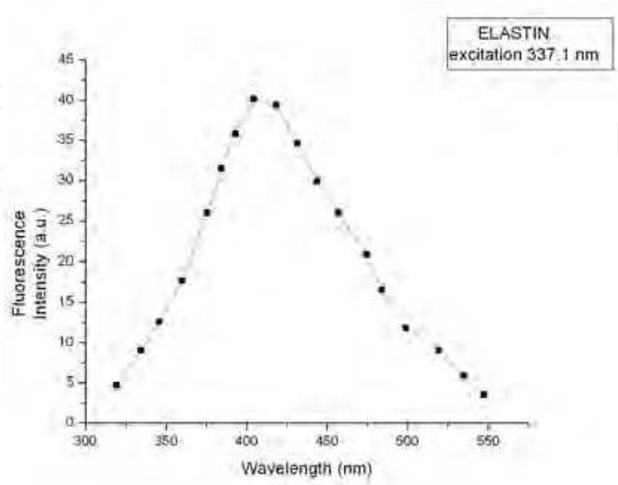

Fig. 9. Fluorescence emitted by elastin excited at 337.1 nm

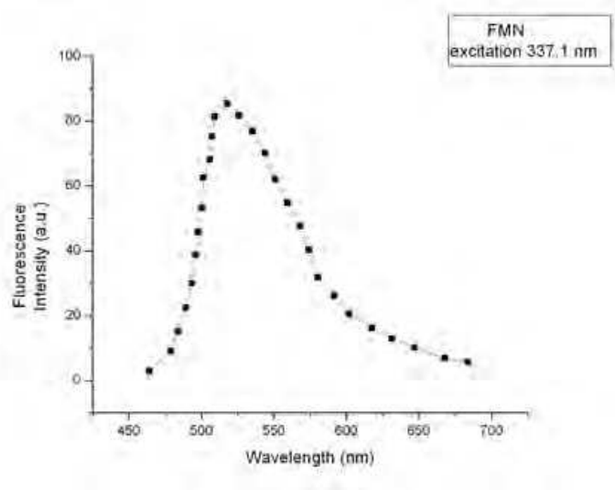

Fig. 10. Fluorescence emitted by FMN

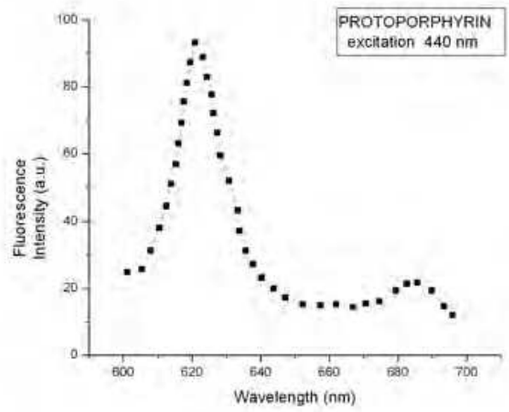

Fig. 11. Fluorescence emission of riboflavin

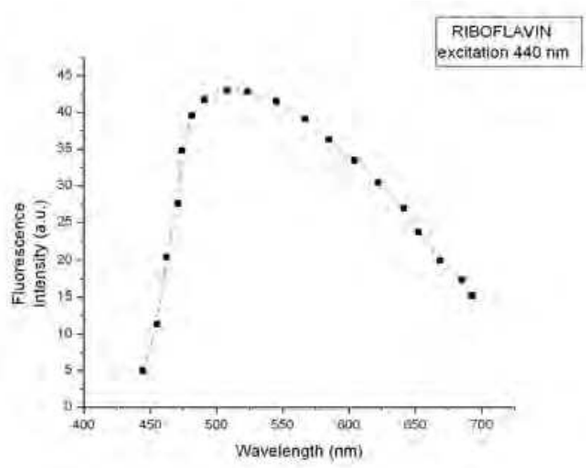

Fig. 12. Fluorescence emission of protoporphyrin

The results are given in Table 2, which shows the fluorescence peak positions, together with the corresponding excitation wavelengths.

Compound	Solvent / concentration	Excitation wavelength (nm) / utilized laser	Fluorescence wavelength peak
Collagen	10^{-5}M phosphate buffer aqueous solutions at pH = 7	270/SHG of dye laser at 540 nm	395
Collagen	10^{-5}M phosphate buffer aqueous solutions at pH = 7	285/SHG of dye laser at 570 nm	310
Collagen	10^{-5}M phosphate buffer aqueous solutions at pH = 7	337.1/NPL	395
NADH	10^{-5}M phosphate buffer aqueous solutions at pH = 7	290/SHG of dye laser at 580 nm	510
NADH	10^{-5}M phosphate buffer aqueous solutions at pH = 7	337.1/NPL	455
NADH	10^{-5}M phosphate buffer aqueous solutions at pH = 7	400/tunable dye laser (POPOP)	510

Table 2. Fluorescence peaks of several fluorophores

The lifetimes of the fluorescence radiation emitted by some fluorophores that are found in the brain tissues, measured as in Fig.2, are displayed in Table 3; most of the values are between 1ns and 10ns. As for NADH this value is very short and a p-i-n (PIN) fast photodiode was used, which was able to indicate only that the fluorescence lifetime is shorter than 0.5 ns. On the contrary for the FMN the lifetime is longer, around 45ns.
These values may be used as discriminating factors between different types of tissues.

Compound	Fluorescence lifetime (FTWHM) ns	Compound	Fluorescence lifetime (FTWHM) ns
Tryptophan	2.9	Collagen	5.5
Tyrosine	4.1	Flavin monocleotide (FMN)	45
Phenylalanine	6.0	Porphyrin	12
NADH	< 0.5		

Table 3. Fluorescence lifetimes for several brain tissue compounds

The autofluorescence measurements performed on some of the main molecular components of the brain tissues allow to conclude as follows: (a) the autofluorescence spectra of the fluorophores strongly depend on the absorption characteristics of the fluorophores molecules, which–in turn–depend on the solvent, solution pH, and concentrations in the samples; this is a rather general conclusion in LIF but, in this case, it becomes particularly critical; (b) the fluorescence excitation and emission spectra are mainly obtained by excitation with laser radiation in the near-ultraviolet and visible (200–500 nm) and are emitted in the visible; (c) each of the fluorophore molecules has a specific fluorescence pattern/trace which depends on the excitation wavelength. The spectral distribution of the fluorescence radiation and the number, relative intensities and shapes of the peaks are strongly dependent on the excitation wavelength. For qualitative analysis, the use is

recommended of more successive wavelengths in order to accurately identify the specific peaks for each fluorescence source; (d) if fluorescence peaks, that are very close to each other in the spectrum, are emitted by different fluorophores, one possibility to reveal the emitting molecules and to differentiate between them is to measure the fluorescence lifetime, which may differ from one fluorophore to another.

3.2 Brain tissue measurements

The data reported above can be used to reveal alterations of normal brain tissues towards tumor tissues (either benign or malignant). For such cases, the first factors to be considered are related to the interaction between the laser beam and the tissue on which it is falling (Pascu, 2000; Danaila and Pascu, 2001; Pascu et al., 2009). Figure 13 describes the processes of laser beam interaction with brain tissues which derive from the general case of the laser beam-target tissues interaction. At the point of contact with the tissue border (i.e. the interface of the tissue with the environment form which the laser beam comes), the laser beam (of intensity I_0) is reflected in part (I_R) and backscattered ($I_{b.s}$) by elastic scattering (Gong et al., 2008); a non-negligible part of it is sent back to the environment without interacting with the tissue. The beam penetrating the tissue is refracted (I_r), depending on the tissue's optical properties and changes its propagation direction with respect to the incident beam. A part of it is scattered forward ($I_{f.s}$) the light spreading around the incidence point inside the tissue in all directions, function of the unhomogeneities of the tissue. Another part (I_a) is absorbed by resonant interaction. The rest (I_{rem}) propagates further into the tissue. The energy balance is given by:

$$I_0 = I_R + I_{b.s.} + I_r + I_{f.s.} + I_a + I_{rem.}$$

The equation above is approximate since it does not take into account the inelastic scattering of the laser light which may take place in the tissue; I_a describes not only the laser beam intensity absorbed along the main propagation line (which is mainly defined by the refracted beam direction) but also the absorption which takes place in all the tissue volume, scattered light included.

Out of the mentioned intensities, I_a is responsible for the excitation of the autofluorescence radiation. At the wavelengths used in these studies, water and hemoglobin (two important components of brain tissues) do not interfere with the fluorescence emission process. Water is practically nonabsorbing in the visible and the near-ultraviolet absorption does not lead to fluorescence emission by water molecules.

Hemoglobin does not absorb above 600 nm, and the strong absorption below 600 nm does not lead to significant fluorescence emission (hemoglobin fluoresces very weakly when excited below 300 nm, and the fluorescence lifetime is shorter than 25 ps). Even so, brain tissue samples not having blood within the structure (because they were abundantly washed with natural saline solution) were chosen for the study so that absorption of the laser beam due to hemoglobin in the samples was negligible. Autofluorescence of the tissue samples was excited at 337.1 nm and at longer wavelengths, up to 500 nm.

These wavelengths are also recommended for in vitro measurements for other reasons: the depth of laser beam penetration in the tissue is much lower (one-two orders of magnitude) below 337 nm, the radiation at 337.1 nm and above this wavelength is more intense (typically one order of magnitude higher) than in the case of beams (available for these studies) emitted below 300 nm; in vivo interaction of the brain tissues with radiation below

300 nm may lead to undesirable effects on the cells, such as cleavage of molecular bonds (Lin et al., 2001).

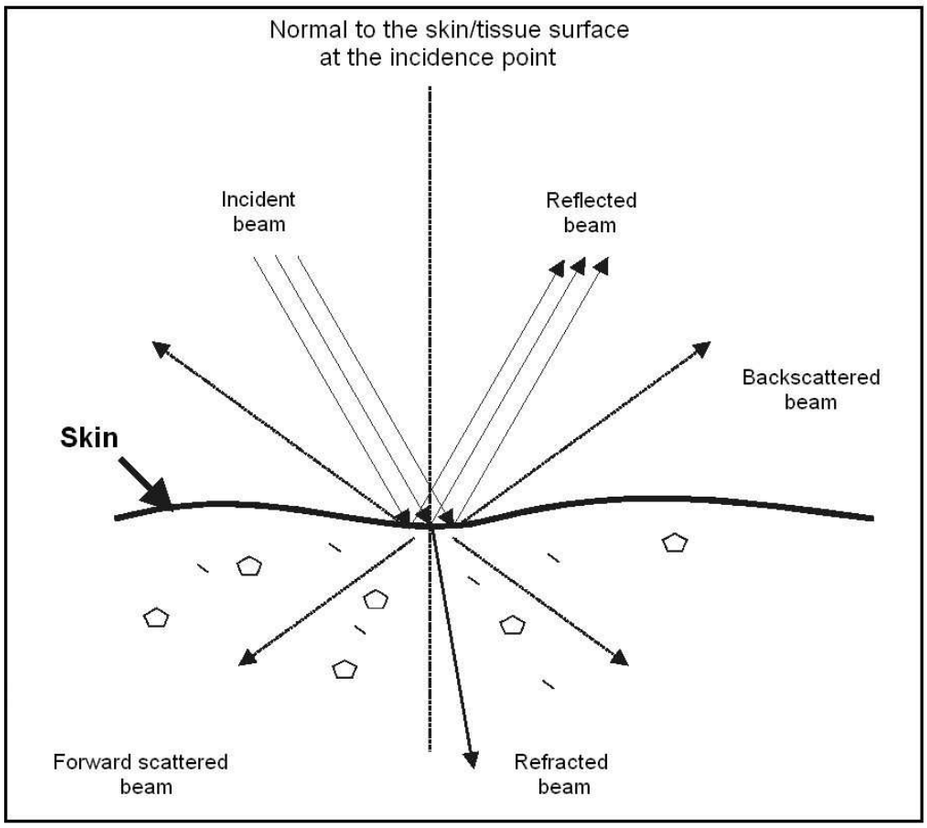

Fig. 13. Laser beam-tissue coupling processes

The excitation at the mentioned wavelengths allows to include contributions to the autofluorescence spectrum of all the fluorophores contained in the brain tissues (Drezek et al., 2001a,b; Trujillo et al., 1998). Since in vitro measurements were made in brain tissue samples extracted under anesthesia, the fluorescence properties of the utilized anesthetics were considered as well. The substances were sodium thiopental, fentanyl, pancuronium, suxamethonium, and sevoflurane. Following excitation, sodium thiopental, pancuronium, and fentanyl do not show fluorescence emission. Suxamethonium affects the tryptophan side-chain chromophores, and sevoflurane quenches tryptophan fluorescence and reversibly increases NADH fluorescence (Ramanujam et al., 1994; Utzinger et al., 1999). The anesthetics are distributed in both normal brain tissue and the tumor, so that their contribution to the autofluorescence spectrum may be detected in both cases. It might be that their concentration in the tumor is higher, in which case LIF signals would be stronger on the tumor side, so that the edge between the normal tissue and the tumor could be more precisely identified.

The tumor samples used for in vitro measurements were extracted by neurosurgical operations performed according to current medical procedures. The normal tissue samples were taken (using standard procedures) from zones around nonruptured aneurisms that

had been operated to prevent accidental ruptures. The measurements were made in tissue samples extracted from different brain tumors. A set of tumors and their location in the brain as shown in the CT or MRI images are given in Figs. 14 - 17, which show the brain status before and after tumor extraction.

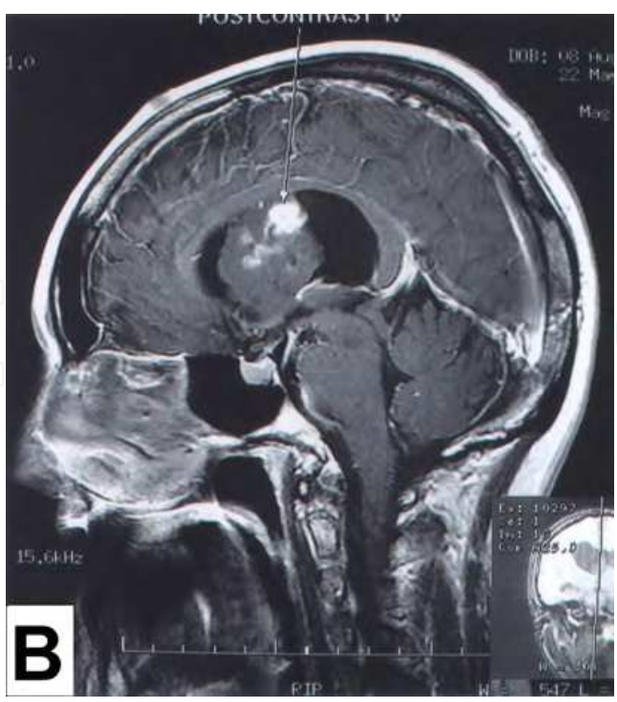

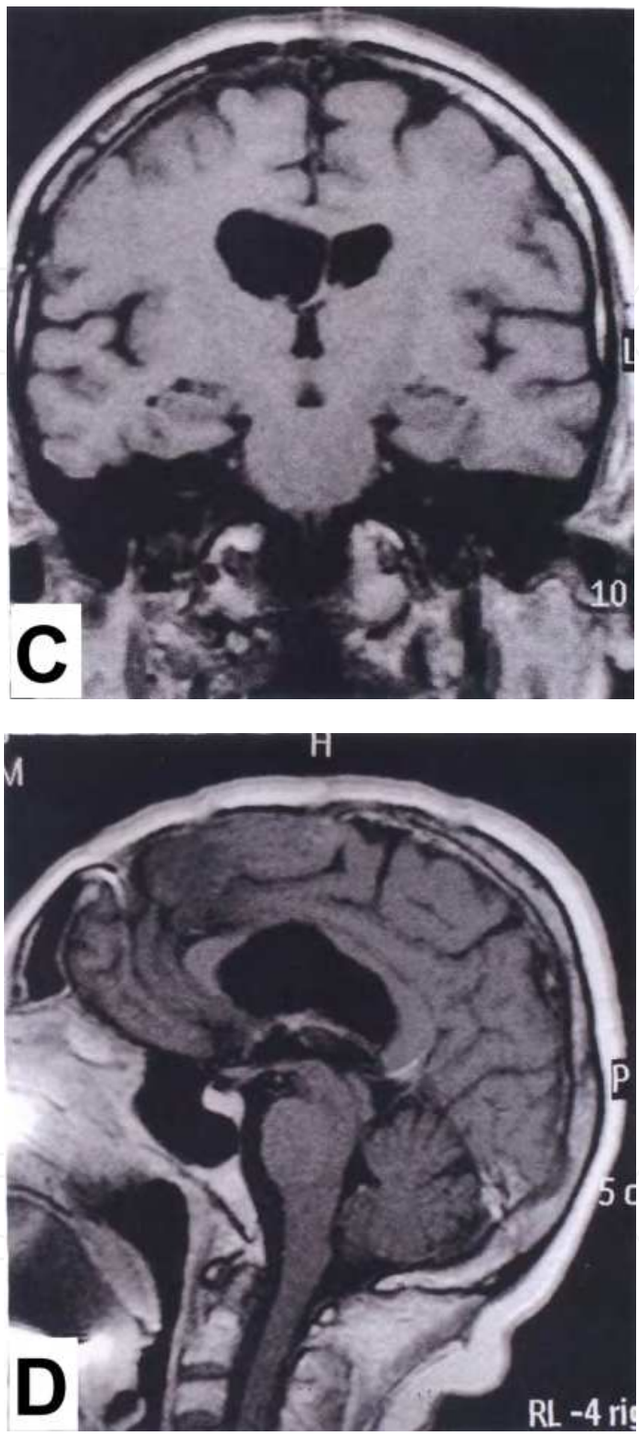

Fig. 14. A and B: Preoperative coronal and sagital T1-weight gadolinium-enhanced MRI, demonstrating of an anterior third ventricle tumor (astrocytoma); C and D: Images obtained after complete removal of the tumor making excision thorugh a midline transcallosal approach (surgeon Leon Danaila).

A typical autofluorescence curve for a normal tissue excited at 337.1 nm is shown in Fig. 18, measured under the conditions specified in paragraph 2.3.2; the emission peak is located at 460– 470 nm, and the curve shape shows a possible contribution of NADH, flavin, and porphyrin. Similar autofluorescence spectra were measured in different samples of normal brain tissue, excited at 337.1 nm. The curves are slightly different from each other, which show a relative variability and a low reproducibility of the autofluorescence signals from one patient to another. The differences may be due to the different optical properties of the tissues (the relative concentrations of the fluorophores in them, the pH, and the different homogeneity). The detailed studies of a large number of autofluorescence spectra of normal brain tissues excited in the visible and ultraviolet allow the conclusion that the autofluorescence of a brain tissue is not a mathematical sum of the contributions of the fluorophores existing in its structure, because (a) the autofluorescence peaks are quite broad, which makes it difficult to accurately estimate their wavelengths; (b) the different wavelengths to use for autofluorescence excitation (around 340 nm and particularly 337.1 nm) are most recommended due to relatively deeper penetration of the radiation in the tissues and at these wavelengths most fluorophores yield marked fluorescence signals; and (c) spectra differ, although not dramatically, from one brain zone to another and from one patient to another, even under strictly reproducible experimental conditions. These conclusions suggest that in order to use LIF for distinguishing between normal brain and (malignant) tumor tissues in real-time neurosurgical operations, ''in situ'' measurements for normal/tumor tissue pairs should be made. This could enable a correct evaluation of the tumor boundaries with respect to the normal tissues for each specific case.

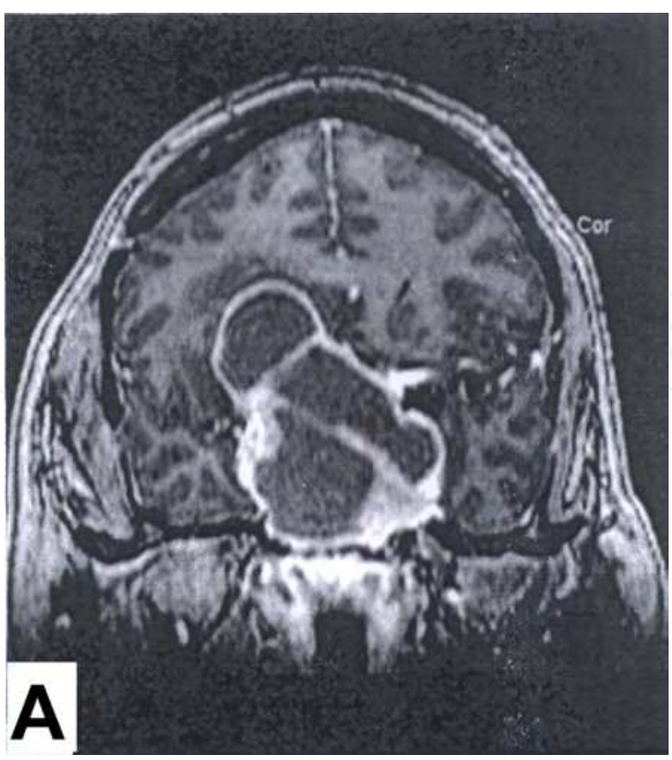

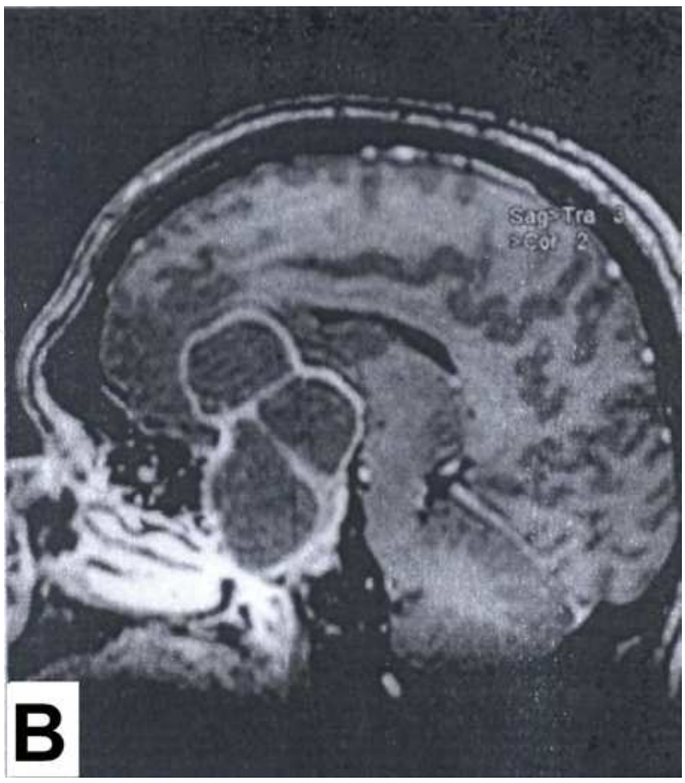
B

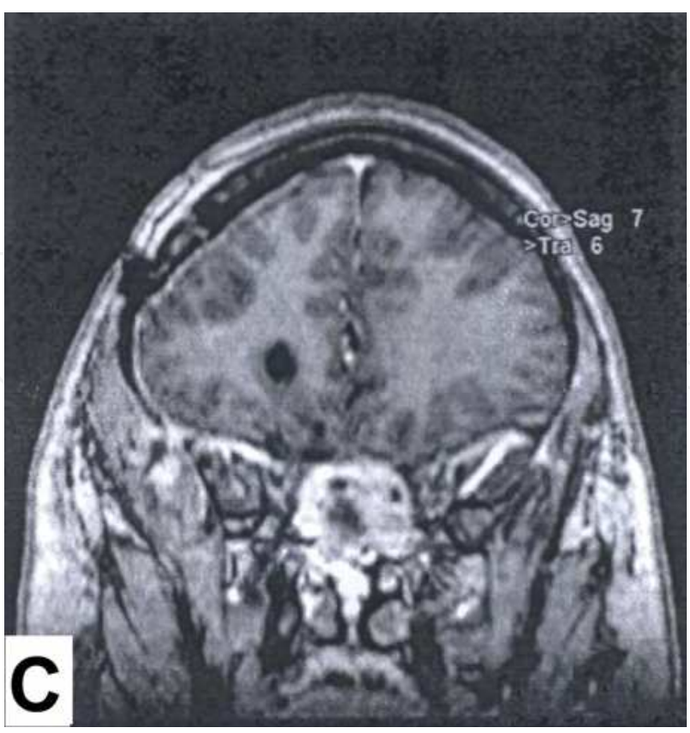
C

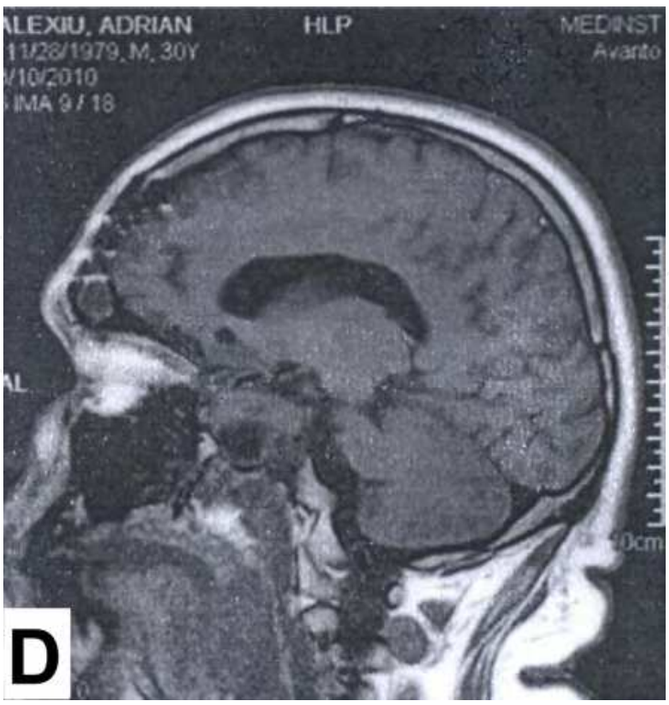

Fig. 15. A and B: Preoperative contrast –enhanced ,T1 –weighted, coronal and sagital MRI scan demonstrated hypointense sellar and suprasellar polycystic lesion a rim of cysts walls enhancement and a region of intracyst enhancement; C and D: T1-weighted coronal and surgical MRI after radical subfrontal resection (surgeon Leon Danaila).

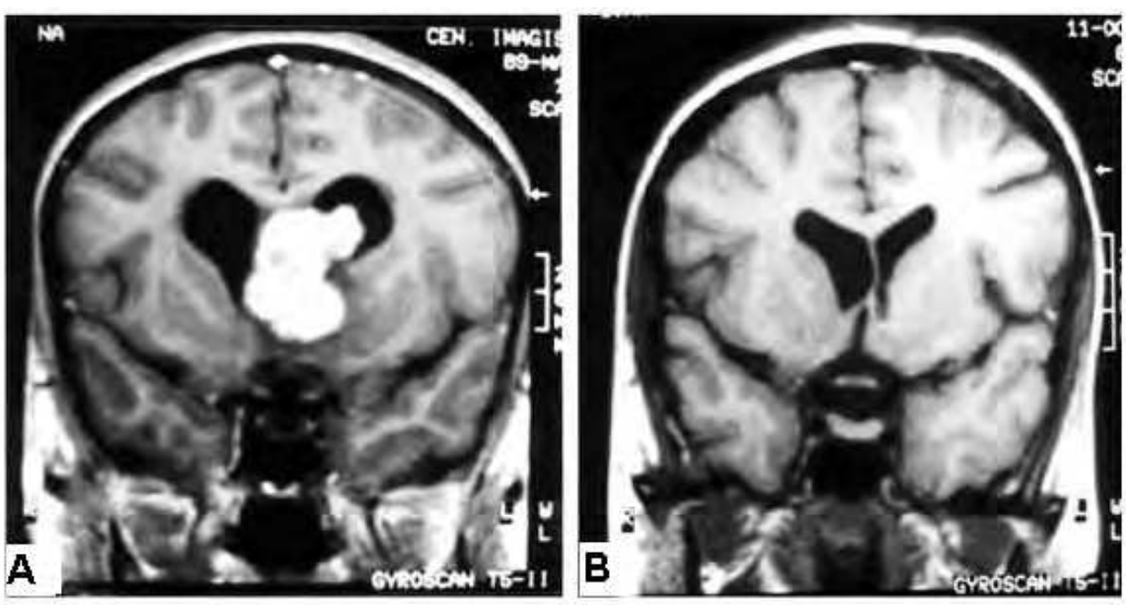

Fig. 16. Large left intraventricular astrocytoma. A: Preoperative contrass-enhanced coronal magnetic resonance imaging scan. B. Postoperative contrast-enhanced resonance imaging scan (surgeon Leon Danaila).

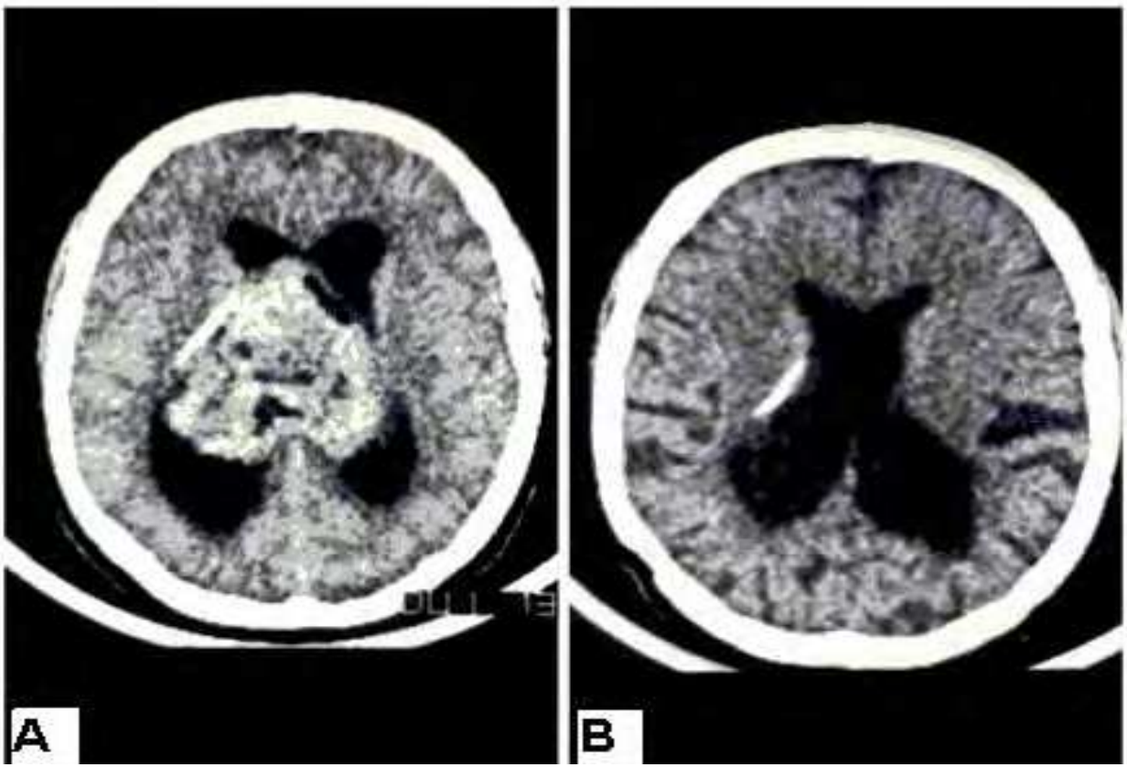

Fig. 17. Intraventricular astrocytoma. A: Preoperative contrast-enhanced axial CT scan demonstrates a heterogeneously enhancing tumor within the lateral ventricle. The patient underwent craniotomy and resection of this tumor through parieto-occipital approach. B: Postoperative CT scan demonstrates resection of the tumor (surgeon Leon Danaila).

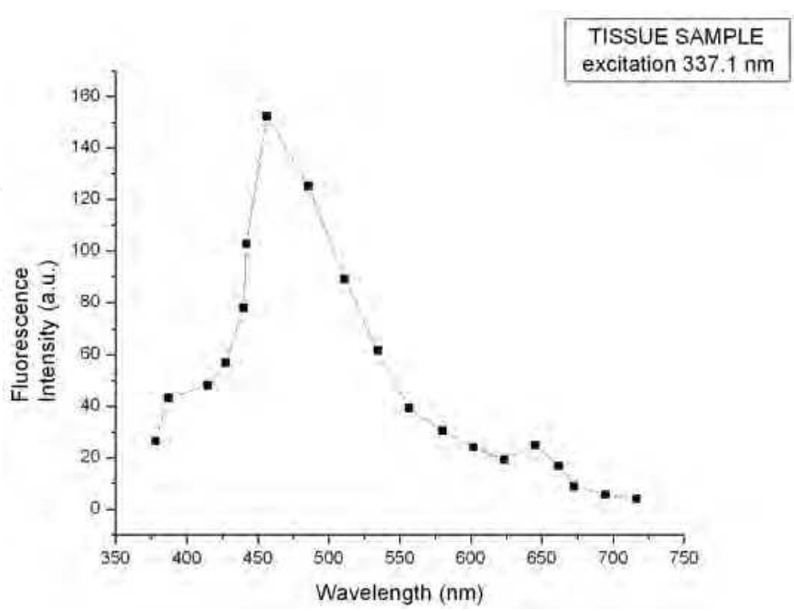

Fig. 18. The autofluorescence emission of a normal brain tissue excited at 337.1 nm.

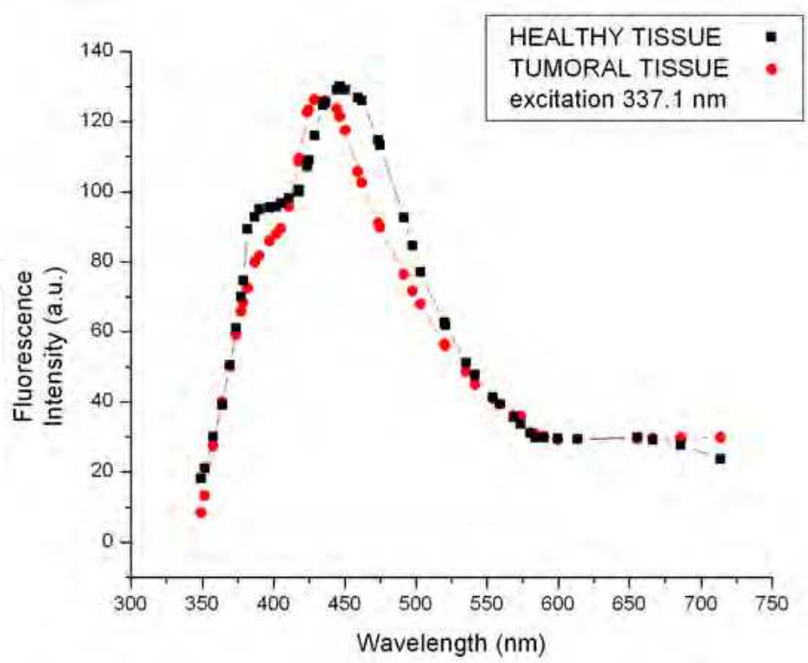

Fig. 19. The autofluorescence emission of a healthy brain tissue and of a barin malignant tumor tissue excited at 337.1 nm.

3.3 Autofluorescence of normal/tumor brain tissue pairs

Measurements were performed on several sample pairs (prepared as mentioned in the 2.3.2 paragraph), each pair consisting of tumor tissue and normal tissue extracted from the same patient. The normal tissue samples were prelevated to avoid zones of brain compression by the tumor. In collecting the samples, different kinds of tumor were chosen, so that the nature of the tumor was not a criterion in selecting the tissues to analyze. Given the fluorophores present in the structure of the brain tissues, and their autofluorescence properties, three wavelengths were selected to excite the autofluorescence: 337.1, 370, and 410 nm.

The measurements performed on homogenates showed that (a) the spectral distribution of the autofluorescence signals for a given homogenate is very close to that of the untreated sample and it is reproducible from one measurement to another; and (b) the autofluorescence spectra of the tumor samples are close to those of normal tissues, but the differences that do exist between them enable identification of the tumor and the normal tissue and consequently their differentiation. The main difference is that for each sample pair the peak autofluorescence spectrum for the normal tissue is shifted with respect to the tumor case. The overall intensity of the autofluorescence is also different for the components of the pair. As an example, Fig. 19 shows the autofluorescence of a normal sample excited at 337.1 nm and the spectrum obtained under the same conditions for the tumor sample. Comparison of the two curves illustrates that the autofluorescence peaks are shifted by 15 nm. The two autofluorescence peaks for the normal tissue are emitted at 390 and 450 nm, the intensity ratio being: $R_{337normal} = I_{450} / I_{390} = 1.44$; for the tumor sample, $R_{337tumor} = I_{450} / I_{390} = 1.31$. Another parameter measured to individualize the autofluorescence curves is the overall intensity, defined as $I_{overall} = \int I(\lambda)$. It is specific for each curve, and is a function of the pumping wavelength. For Fig. 19, $I_{337normal} = 18.298$, respectively, $I_{337tumor} = 12.852$. The

above-mentioned quantities (the peak intensity walk-off, the ratio between the main fluorescence peaks, and the overall autofluorescence intensity) may be used as objective parameters to differentiate between normal and tumor brain tissues. For excitation of the samples at 337.1 nm, these parameters differ from the normal to the tumor tissue by 15 nm peak intensity walk-off, 10% variation of the ratio of the peak intensities, and about 40% difference in the overall autofluorescence intensity. The same kind of measurement is made for samples excited at 370 nm. Figure 20 shows the autofluorescence spectra for the normal and tumor samples. The peak intensity ratios for 470 and 525 nm are $R_{370normal} = I_{470} / I_{525} = 1.51$; $R_{370tumor} = I_{470} / I_{525} = 2.09$; the difference is about 40%. Thus, $I_{370normal} = 20.2$ and $I_{370tumor} = 16.4$, a difference of 23%. For the excitation at 410 nm, the obtained autofluorescence spectra are shown in Fig. 21; the respective parameters are $R_{410normal} = 1.45$ and $R_{410tumor} = 2.15$, the difference being 40%;

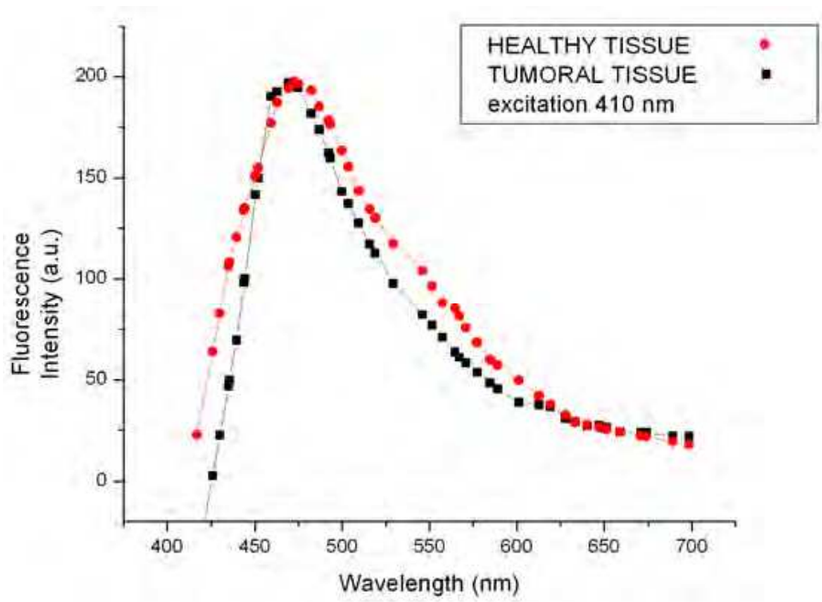

Fig. 20. The autofluorescence spectra for healthy and malignant tumor brain samples (excitation at 410 nm).

$I_{410normal} = 10.52$ and $I_{410tumor} = 16.125$, the difference being 27%.

Another parameter that may be used to distinguish between the normal and the tumor tissue is what we called the quality factor of the fluorescence curve, Q, defined as the ratio between the maximum fluorescence intensity I_{max} and the difference of the two wavelengths where the fluorescence intensity reaches half of its maximum value $\delta\lambda(I_{max}/2)$:

$$Q = I_{max} / \delta\lambda(I_{max}/2)$$

Calculating Q for the curves that represent the fluorescence emission of the two types of tissues at 337.1 nm excitation wavelength (Fig.19), the following values were respectively obtained: $Q_{337norm} = 0.99$ and $Q_{337tum} = 0.67$; these values of the quality factor for the two tissue homogenates differ by about 30%, which qualifies this parameter as a good candidate to describe the spectral differences between the two types of tissue - normal and tumor.

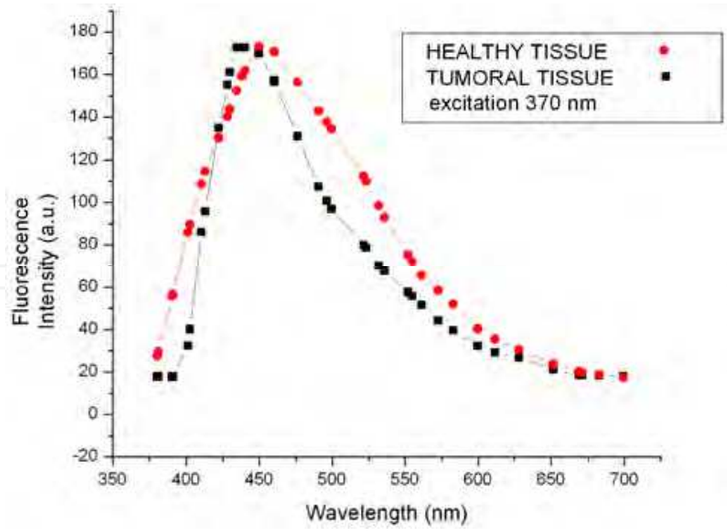

Fig. 21. The autofluorescence spectra for healthy and malignant tumor brain samples (excitation at 370 nm).

Given the fact that:

i. for measuring the pair of the two types of tissue homogenates precautions were taken to insure a reproducible measurement geometry, and

ii. a calibration of the measuring system was performed for each sample measurement the idea of direct subtraction of fluorescence intensity values of the two types of tissue at each wavelength is consistent and do not produce systematic errors.

The result of point by point subtraction of the two autofluorescence curves excited at 337.1 nm shown in Fig.19 is presented as the Figure 22.

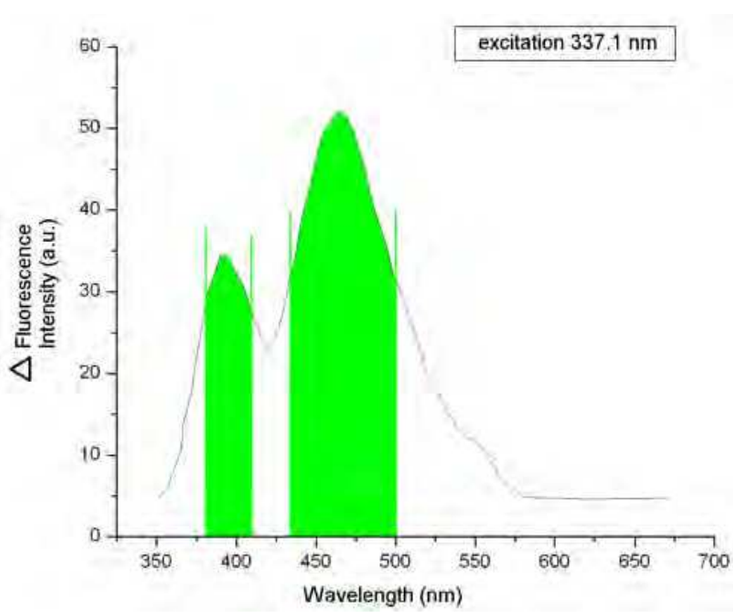

Fig. 22. Difference in autofluorescence spectra between tumor and normal tissue shown in Fig.19. ,Δ Fluorescence Intensity is given in arbitrary units and represents the difference between the autofluorescence signals for each wavelengths .

As results from the Fig. 22, there are two spectral ranges, namely 385 – 415 nm and 460 – 500 nm, within which the difference between the intensity of the fluorescence emitted by the two types of tissue is maximal. This shows the possibility to use this treatment procedure of the pairs of autofluorescence curves to spectrally evidence the difference between the normal and tumor tissue. The difference curve in Fig.22 shows two maxima, at 386 nm and 463 nm wavelengths, respectively. Moreover, at λ = 386 nm the difference of the two intensities is 26% out of the peak of the fluorescence intensity (Fig.19) , while at λ = 463 nm this difference reach even 41% (see Fig.19) , favoring this wavelength. Similar results are obtained from homogenates at excitation wavelengths 370 nm and 410 nm (data not shown).
A summary of all the parameters mentioned in this section (except the subtraction spectrum), computed from the autofluorescence curves obtained for the homogenates of the two types of tissue (normal and tumor) at each of the three excitation wavelengths used, is presented in Table 4.

Excitation Wavelength	**Tissue type**	**Parameter**			
		Ratio R	**Quality factor Q**	**Overall intensity I**	**Walk off of the autofluorescence peak (nm)**
337.1 nm	normal	1.44	0.99	18.298	15.0
	tumor	1.31	0.67	12.852	
370 nm	normal	1.51	1.26	20.2	13.0
	tumor	2.09	1.69	16.4	
410 nm	normal	1.45	1.59	10.52	3.0
	tumor	2.15	1.60	16.125	

Table 4. Summary of the parameters used to differentiate between the normal and tumor tissue samples on the base of autofluorescence spectra

In Table 4 are shown only the results obtained when the autofluorescence is excited, respectively, with 3 wavelengths: 337.1 nm (NPL), 370 nm (SHG starting form the fundamental beam at 540 nm) and 410 nm (POPOP). Of course, during the experiments and tests one may select other wavelengths, namely those that may provide the most important differences between the autofluorescence spectra excited for normal and corresponding tumor brain tissues. Although it appears that the type of tumor does not dramatically influence the measuring techniques, it remains that for each such type, a selection of the most suitable parameter to best monitor the differences is made.

4. Discussion

The reported data, correlated with literature reports (Hogan, 2008; Kremer et al., 2009) show that autofluorescence measurements may constitute a promising method to differentiate between brain tumor tissue and normal brain tissue in the same patient.
In this paper it was demonstrated that by comparing the autofluorescence spectra induced by laser radiation in the ultraviolet and visible, brain tumor and normal tissues can be identified and differentiated. The recommended measurements were not performed on tissue samples kept as they were extracted from the brain, but on homogenates to ensure the

best possible reproducibility of the results. It was concluded that the autofluorescence spectra of the tumor samples are close to those obtained for normal tissues, but there are differences between them that allow distinguishing the tumor from normal tissue.

One difference is that for each tumor/normal tissue sample pair the peak autofluorescence for the normal tissue is translated with respect to that for the tumor, typically between 10 and 20 nm; the overall autofluorescence intensity is different for the components of the same pair, the difference being 15–30%.

Another parameter that may be used is the variation of the ratio of some peaks of fluorescence intensity (which correspond to each other) between the normal and the tumor tissue samples. When this parameter can be measured, the variation range is usually between 10% and 40%.

A specific factor that may be used to differentiate between normal and tumor brain tissues is the quality factor of the autofluorescence curves which may vary in the range 1 to 2 for normal tissues and from 0.5 to 1.6 for tumor tissues, function of the laser beam wavelength used to excite the fluorescence.

As for the difference spectra obtained by subtracting the autoflorescence signals in the normal, respectively tumor case, the peaks which are obtained could be used to distinguish between to the types of tissues in real time; on the other hand, it remains to chose the most recommended wavelength to excite the fluorescence, so that the difference spectra exhibit the best resolution of the difference peaks.

Another conclusion is that in vitro experiments show that for the measurements, it is mandatory to use normal /tumor tissue sample pairs taken from the same patient. In our case, for ethical considerations, the samples used were extracted from the brain during medically justified neurosurgical operations, in agreement with operative standards. For studies on normal tissues only, the samples were extracted from normal tissues affected by nonruptured aneurisms in patients who were different from the patients exhibiting malignant brain tumors. The results show that the method may be adapted, after further experimental in vitro tests, to real-time intraoperative conditions by measuring the autofluorescence of the tumor and of the adjacent normal tissue; to do that, it is first necessary to consider the effect of tumor pressure on the molecular content and structure of the adjacent normal tissues. Because real-time investigation does not require tissue extraction, the method could be acceptable to the ethics bodies supervising neurosurgical operations; intraoperative fluorescence guidance for resection of malignant tumors is currently receiving more clinical interest both for imaging purposes (Kantelhardt et al., 2007) and for fast intraoperative diagnostics (Croce et al., 2003; Kremer et al., 2009). The results reported in this paper demonstrate that for neurosurgical clinical use of autofluorescence measurements, the following precautions should be taken: (a) the autofluorescence measurements, either in vitro or in vivo, should be made using tissue pairs: normal/malignant tumor; (b) the contribution of any anesthetic to the measured autofluorescence should always be evaluated, to avoid unexpected interference with the natural autofluorescence of the tissues and errors in data interpretation; the fluorescence emitted by exogenous fluorophores which might be present in the brain area submitted to autofluorescence screening should also be carefully evaluated; (c) in obtaining the autofluorescence spectra, the optimal intensity of the laser excitation beam should be chosen to prevent both damage to the brain tissues and the quadratic Stark broadening of the absorption and fluorescence bands; the latter might induce errors in the accurate measurement of the peak wavelengths and of the overall fluorescence bands.

5. Acknowledgements

The authors would thank Mr. Ionut Relu Andrei for help in processing the CT and MRI images. They acknowledge the funding of this work by VIASAN project No. 125/2001 and ANCS LAPLAS-3/2009 project.

6. References

Andersson-Engels, S.; Brun, A.; Kjellén, E.; Salford, L. G.; Strömblad, L. G.; Svanberg, K.; Svanberg, S. (1989). Identification of brain tumors in rats using laser-induced fluorescence and haematoporphyrin derivative, *Lasers in Medical Science*, Vol. 4, No. 4, pp.241-249.

Andersson-Engels, S.; Johansson, J.; Stenram, U.; Svanberg, K.; Svanberg, S. (1990a). Malignant tumor and atherosclerotic plaque diagnosis using laser-induced fluorescence, *IEEE J Quant. Electronics*, Vol.26, Iss 12, pp.2207-2217. doi: 10.1109/3.64357.

Andersson-Engels, S.; Johansson, J.; Stenramb, U.; Svanberg, K.; Svanberg, S. (1990b). Time-resolved laser-induced fluorescence spectroscopy for enhanced demarcation of human atherosclerotic plaques, *J. Photochem. Photobiol. B: Biology*, Vol. 4, Iss. 4, pp. 363-369. doi:10.1016/1011-1344(90)85015-O

Andersson-Engels, S.; Johansson, J.; Svanberg, S. (1994). Medical diagnostic system based on simultaneous multispectral fluorescence imaging, *Appl Opt*, Vol. 33, pp. 8022-8029. doi:10.1364/AO.33.008022.

Ankerst, J.; Montán, S.; Svanberg, K.; Svanberg, S. (1984). Laser-Induced Fluorescence Studies of Hematoporphyrin Derivative (HPD) in Normal and Tumor Tissue of Rat, *Appl. Spectrosc.* , Vol. 38, pp.890-896.

Bottiroli, G.; Croce, A.; Locatelli, D.; Nano, R.; Giombelli, E.; Messina, A.; Benericetti, E. (1998). Brain tissue autofluorescence: an aid for intraoperative delineation of tumor resection margins. *Cancer Detect Prev*, Vol. 22, No.4, pp. 330–339.

Brewer, M.; Utzinger, U.; Silva, E.; Gershenson, D.; Bast, R. C.; Follen, M.; Richards-Kortum, R. (2001). Fluorescence Spectroscopy for In Vivo Characterization of Ovarian Tissue *Lasers in Surgery and Medicine*, Vol. 29, pp.128-135.

Butte, P. V.; Fang, Q.; Jo, J. A.; Yong, W. H.; Pikul, B. K.; Black, K. L.; Marcu, L. (2010). Intraoperative delineation of primary brain tumors using time-resolved fluorescence spectroscopy, *J Biomed Opt* , Vol.15, pp. 027008. doi:10.1117/1.3374049.

Butte, P.V.; Mamelak, A.N.; Nuno M.; Bannykh S. I.; Black K.L.; Marcu L.(2011).Fluorescence lifetime spectroscopy for guided therapy of brain tumors, *NeuroImage,* Vol. 54, pp. S125–S135.

Croce, A. C.; Fiorani, S.; Locatelli, D.; Nano, R.; Ceroni, M.; Tancioni, F.; Giombelli, E. (2003). Diagnostic potential of autofluorescence for an assisted intraoperative delineation of glioblastoma resectionmargins, *Photochem Photobiol*, Vol. 77, pp.309–318.

Cubillos, S.; Obregon, F.; Vargas, M. F.; Salazar, L. A.; Lima, L. (2006). Taurine concentration in human gliomas and meningiomas: tumoral, peritumoral and extratumoral tissue, *Adv Exp Med Biol* , Vol. 583, pp. 419–422.

Danaila, L. & Pascu, M. L. (1999). Photodynamic therapy of the cerebral malignant tumors, *Rom J Biophys* , Vol. 10, pp.:145–152.

Danaila, L. & Pascu, M, L. (2001). Lasers in neurosurgery. Bucharest: Academia Romana. ISBN 973-27-0802-6.

Drezek, R.; Sokolov, K.; Utzinger, U.; Boiko, I.; Malpica, A.; Follen, M.; Richards-Kortum , R. (2001a). Understanding the contributions of NADH and collagen to cervical tissue fluorescence spectra: modeling, measurements, and implications. J *Biomed Opt* , Vol.6, pp.385–396.

Drezek, R.; Brookner, C.; Pavlova, I.; Boiko, I.; Malpica, A.; Lotan, R.; Follen, M.; Richards-Kortum ,R. (2001b). Autofluorescence microscopy of fresh cervical-tissue sections reveals alterations in tissue biochemistrywith dysplasia. *Photochem Photobiol* , Vol.73, pp.636–641.

Gebhart, S. C.; Majumder, S. K.; Mahadevan-Jansen, A. (2006). Spectral Imaging for Brain Tumor Margin Demarcation, in *Biomedical Optics*, Technical Digest (CD) (Optical Society of America, 2006), paper SG5.

Gong, J.; Yi, J.; Turzhitsky, V. M.; Muro, K.; Li, X. (2008). Characterization of malignant brain tumor using elastic light scattering spectroscopy, *Disease Markers* , Vol. 25, No.6, pp.303-312.

Hogan, H. (2008). Mapping molecular highways: second harmonic generation reveals polarity in neurons, *Biophoton Int* October, pp. 36–37.

Kantelhardt, S. R.; Leppert, J.; Krajewski,; Petkus, N.; Reusche, E.; Tronnier, V. M.; Hüttmann, G.; Giese, A. (2007). Imaging of brain and brain tumor specimens by time-resolved multiphoton excitation microscopy ex-vivo. *Neuro Oncol* , Vol.9, pp.103–112.

Kremer P.; Mahmoudreza, F.; Ding, R.; Pritsch, M.; Zouba, S.; Frei E. (2009). Intraoperative fluorescence staining of malignant brain tumors using 5-aminofluorescein-labelled albumin, *Oper Neurosurg* , Vol. 64, pp.53–61.

Lin, W.-C.; Toms, S. A.; Motamedi, M.; Jansen, E. D.; Mahadevan-Jansen, A. (2000). Brain tumor demarcation using spectroscopy: an in vitrostudy, *J Biomed Opt* , Vol.5, pp.214–220.

Lin, W.-C.; Toms, S. A.; Johnson, M.; Jansen, E. D.; Mahadevan-Jansen, A. (2001). In vivo brain tumor demarcation using optical spectroscopy, *Photochem Photobiol* , Vol.73, pp. 396–402.

Lin, W.-C.; Mahadevan-Jansen, A.; Jansen, E. D.; Toms, S. A.; Steven, A. (2002). Tumor demarcation using optical spectroscopy. *US Pat. 6,377,841.*

Marcu, L.; Jo, J. A.; Butte, P. V.; Yong, W. H.; Pikul, B. K.; Black, K. L.; Thompson ,R. C. (2007). Fluorescence Lifetime Spectroscopy of Glioblastoma Multiforme, *Photochem and Photobiol* , Vol.80, Iss.1, pp.98-103; doi: 10.1111/j.1751-1097.2004.tb00055.

Montán, S.; Svanberg, K.; Svanberg, S. (1985). Multicolor imaging and contrast enhancement in cancer-tumor localization using laser-induced fluorescence in hematoporphyrin-derivative-bearing tissue, *Optics Letters*, Vol. 10, Iss. 2, pp. 56-58. doi:10.1364/OL.10.000056.

Pascu, M. L. (2000). Laser physics. In: Simunovic Z, editor. *Lasers in medicine and dentistry*, Rijeka, Croatia: Vitagraaf d. o. o. ISBN 953-6059-30-4.

Pascu, A.; Romanitan, M. O.; Delgado, J. M.; Danaila, L.; Pascu, M. L. (2009). Laser-induced autofluorescence measurements on brain tissues, *Anatomical Record* , Vol.292, pp. 2013–2022.

Ramanujam, N.; Mitchell, M. F.; Mahadevan, A.; Warren, S.; Thomsen, S.; Silva, E.; Richards-Kortum, R. (1994). In vivo diagnosis of cervical intraepithelial neoplasia using 337-nm-excited laser-induced fluorescence, *Proc Natl Acad Sci USA*, Vol.91, pp.10193–10197.

Ramanujam, N. (2000). Fluorescence spectroscopy in vivo. In: Meyers RA, editor. *Encyclopedia of analytical chemistry,* Chichester: Wiley. pp. 20–56.

Sokolov, K.; Follen, M. M.; Richards-Kortum, R. (2002). Optical spectroscopy for detection of neoplasia, *Curr Opin Chem Biol* , Vol. 6, pp. 651–658.

Sun, Y.; Hatami, N.; Yee, M.; Phipps, J.; Elson, D. S.; Gorin, F.; Schrot, R. J.; Marcu, L. (2010). Fluorescence lifetime imaging microscopy for brain tumor image-guided surgery, *J Biomed Opt* , Vol. 15, pp. 056022. doi:10.1117/1.3486612.

Svanberg, K & Svanberg, S. (1983). Diagnostics and treatment of cancer tumors based on photoactivation of hematoporphyrin derivative (HpD) - A literature survey, Literature survey, Lund Institute of Technology, *Lund Reports on Atomic Physics* LRAP-23, Sweden.

Svanberg, K.; Kjellén, E.; Ankerst, J.; Montán, S.; Sjöholm, E.; Svanberg, S. (1986). Fluorescence studies of hematoporphyrin derivative (HpD) in normal and malignant rat tissue, *Cancer Res.* , Vol. 46, pp. 3803-3808.

Svanberg, S.(1987). Medical diagnostics using laser-induced fluorescence, *Physica Scripta,* Vol. T19, pp.469-475.

Toms, S. A.; Lin, W. C.; Weil, R. J.; Johnson, M. D.; Jansen, E. D.; Mahadevan-Jansen, A. (2005). Intraoperative Optical Spectroscopy Identifies Infiltrating Glioma Margins with High Sensitivity, *Neurosurgery* , Vol.57, Iss 4, pp. 382-391. doi: 10.1227/01.NEU.000176855.39826.2D.

Trujillo, E. V.; Sandison, D. R.; Utzinger, U.; Ramanujam, N.; Follen-Mitchell, M.; Richards-Kortum, R. (1998). Method to determine tissue fluorescence efficiency in vivo and predict signal-to-noise ratio for spectrometers, *Appl Spectrosc* , Vol. 52, pp. 943–951.

Utzinger, U.; Trujillo, E. V.; Atkinson, E. N.; Mitchell, M. F.; Cantor, S. B.; Richards-Kortum, R. (1999). Performance estimation of diagnostic tests for cervical precancer based on fluorescence spectroscopy: effects of tissue type, sample size, population, and signal-to-noise ratio, *IEEE Trans Biomed Eng,* Vol.46, pp. 1293–1303.

Valeur, B. (2001). Molecular fluorescence: principles and applications. Weinheim: Wiley.

Wu, T.; Qu, J. Y. ; Cheung, T.-H.; Lo, K. W.-K. (2003). Preliminary study of detecting neoplastic growths in vivo with real-time calibrated autofluorescence imaging, *Opt Exp* , Vol.11, pp. 291–298.

Yong, W.; Butte, P. V.; Pikul, B. K.; Jo, J. A.; Fang, Q.; Papaioannou, T.; Black, K. L.; Marcu, L. (2006). Distinction of brain tissue, low-grade and high-grade glioma with time-resolved fluorescence spectroscopy, *Front Biosci* , Vol. 11, pp. 1255–1263.

Zuluaga, A. F.; Utzinger, U.; Durkin, A.; Fuchs, H.; Gillenwater, A.; Jacob, R.; Kemp, B.; Fan, J.; Richards-Kortum, R. (1999). Fluorescence excitation emission matrices of human tissue: a system for in vivo measurement and method of data analysis, *Appl Spectrosc* , Vol. 53, pp. 302–311.

IntechOpen

IntechOpen

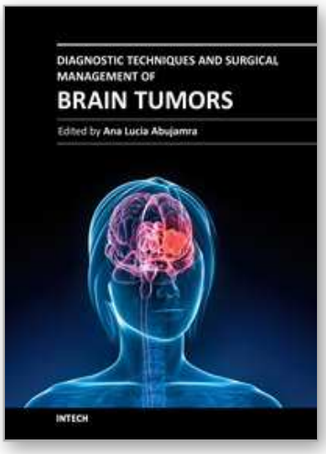

Diagnostic Techniques and Surgical Management of Brain Tumors
Edited by Dr. Ana Lucia Abujamra

ISBN 978-953-307-589-1
Hard cover, 544 pages
Publisher InTech
Published online 22, September, 2011
Published in print edition September, 2011

The focus of the book Diagnostic Techniques and Surgical Management of Brain Tumors is on describing the established and newly-arising techniques to diagnose central nervous system tumors, with a special focus on neuroimaging, followed by a discussion on the neurosurgical guidelines and techniques to manage and treat this disease. Each chapter in the Diagnostic Techniques and Surgical Management of Brain Tumors is authored by international experts with extensive experience in the areas covered.

How to reference
In order to correctly reference this scholarly work, feel free to copy and paste the following:

Mihail - Lucian Pascu, Mihaela - Oana Romanitan , Alexandru Pascu, Josè - Maria Delgado and Leon Danaila (2011). Laser-Induced Autofluorescence as a Possible Diagnostic Tool for Use in Neurosurgery, Diagnostic Techniques and Surgical Management of Brain Tumors, Dr. Ana Lucia Abujamra (Ed.), ISBN: 978-953-307-589-1, InTech, Available from: http://www.intechopen.com/books/diagnostic-techniques-and-surgical-management-of-brain-tumors/laser-induced-autofluorescence-as-a-possible-diagnostic-tool-for-use-in-neurosurgery

INTECH
open science | open minds

InTech Europe
University Campus STeP Ri
Slavka Krautzeka 83/A
51000 Rijeka, Croatia
Phone: +385 (51) 770 447
Fax: +385 (51) 686 166
www.intechopen.com

InTech China
Unit 405, Office Block, Hotel Equatorial Shanghai
No.65, Yan An Road (West), Shanghai, 200040, China
中国上海市延安西路65号上海国际贵都大饭店办公楼405单元
Phone: +86-21-62489820
Fax: +86-21-62489821

© 2011 The Author(s). Licensee IntechOpen. This chapter is distributed under the terms of the Creative Commons Attribution-NonCommercial-ShareAlike-3.0 License, which permits use, distribution and reproduction for non-commercial purposes, provided the original is properly cited and derivative works building on this content are distributed under the same license.